THE JOURNAL OF BIOLOGICAL CHEMISTRY
Vol. 277, No. 28, Issue of July 12, pp. 25668–25676, 2002

Printed in U.S.A.

The Conserved Helix C Region in the Superfamily of Interferon-γ/Interleukin-10-related Cytokines Corresponds to a High-affinity Binding Site for the HSP70 Chaperone DnaK*

Received for publication, March 27, 2002
Published, JBC Papers in Press, April 22, 2002, DOI 10.1074/jbc.M202984200

Koen Vandenbroeck‡§, Iraide Alloza‡, Dirk Brehmer¶, Alfons Billiau‖, Paul Proost‖, Neil McFerran‡‡, Stefan Rüdiger§§¶¶, and Brian Walker‡**

From the ‡Biomolecular Sciences Research Group, McClay Research Centre for Pharmaceutical Sciences, and the ‡‡Center for Protein and Peptide Engineering, Queen's University of Belfast, Belfast BT9 7BL, United Kingdom, the ¶Institute of Biochemistry and Molecular Biology, University of Freiburg, Freiburg 79104, Germany, the ‖Rega Institute for Medical Research, University of Leuven, Leuven B-3000, Belgium, and the §§Cambridge Centre for Protein Engineering, Medical Research Council Centre, Cambridge CB2 2QH, United Kingdom

HSP70 chaperones mediate protein folding by ATP-dependent interaction with short linear peptide segments that are exposed on unfolded proteins. The mode of action of the *Escherichia coli* homolog DnaK is representative of all HSP70 chaperones, including the endoplasmic reticulum variant BiP/GRP78. DnaK has been shown to be effective in assisting refolding of a wide variety of prokaryotic and eukaryotic proteins, including the α-helical homodimeric secretory cytokine interferon-γ (IFN-γ). We screened solid-phase peptide libraries from human and mouse IFN-γ to identify DnaK-binding sites. Conserved DnaK-binding sites were identified in the N-terminal half of helix B and in the C-terminal half of helix C, both of which are located at the IFN-γ dimer interface. Soluble peptides derived from helices B and C bound DnaK with high affinity in competition assays. No DnaK-binding sites were found in the loops connecting the α-helices. The helix C DnaK-binding site appears to be conserved in most members of the superfamily of interleukin (IL)-10-related cytokines that comprises, apart from IL-10 and IFN-γ, a series of recently discovered small secretory proteins, including IL-19, IL-20, IL-22/IL-TIF, IL-24/MDA-7 (melanoma differentiation-associated gene), IL-26/AK155, and a number of viral IL-10 homologs. These cytokines belong to a relatively small group of homodimeric proteins with highly interdigitated interfaces that exhibit the strongly hydrophobic character of the interior core of a single-chain folded domain. We propose that binding of DnaK to helix C in the superfamily of IL-10-related cytokines may constitute the hallmark of a novel conserved regulatory mechanism in which HSP70-like chaperones assist in the formation of a hydrophobic dimeric "folding" interface.

Interferon-γ (IFN-γ)[1] is a small protein secreted by activated T lymphocytes and natural killer cells. It displays a number of immunoregulatory activities such as activation of macrophages and clonal expansion of $CD4^+$ Th1 lymphocytes, together resulting in a Th1-biased immune response (1). IFN-γ exerts these activities through interaction with and aggregation of a cellular high-affinity receptor consisting of IFN-γ receptor-α and receptor-β chains (2, 3). Ealick *et al.* (4) and Samudzi *et al.* (5) determined the crystal structures of recombinant forms of human and rabbit IFN-γ, respectively. These studies revealed α-helical homodimers, the domains of which consist of six tightly packed α-helices connected by relatively short turns with no β-structure. Four of these helices are donated by one peptide chain and two from the second chain, together constituting a highly intertwined homodimer that is reminiscent of domain swapping (6–8). In particular, the segment helix B-loop II-helix C from one monomer interlocks with extensive interdigitation with the helix E-loop V-helix F segment of the other monomer (4, 5). This dimer interface comprises 35–40% of the total surface area of IFN-γ and is predominantly hydrophobic (4, 5, 9). Taken together, these structural features classify IFN-γ into a small group of homodimeric proteins with hydrophobic, so-called "folding" interfaces, which are presumed to adopt their structure in one step, *i.e.* both chains fold directly into the dimer (10).

It is not known whether the *de novo* folding of IFN-γ into this complex intertwined homodimer structure is a spontaneous process, rather than being strictly dependent on the assistance of chaperones. Circumstantial observations provide support for an assisted process. First, IFN-γ is structurally unstable in that it displays a well documented tendency to aggregate upon exposure to low pH or elevated temperatures (11, 12). *In vitro* aggregation of IFN-γ is an irreversible process that follows first-order kinetics and is thought to occur through a partially folded intermediate structure (12) or via a transiently expanded native species (9, 13). It is likely that such aggregation-prone conformers occur also during folding *in vivo*, thus inferring the need for a biological mechanism for facilitating correct folding and for limiting aggregation. Second, when expressed in *Escherichia coli*, the protein forms inclusion bodies from which bioactive protein can be refolded at the expense of competing

* This work was supported in part by the Allen J. McClay Trust (Belfast, United Kingdom) and by the Fund for Scientific Research of Belgium (Fonds voor Wetenschappelijk Onderzoek-Flanders). The σ^{32}-Q132-Q144-C-IAANS competition assay was performed by D. B. in the laboratory of Bernd Bukau (supported by the Deutsche Forschungsgemeinschaft, Graduiertenkolleg Biochemie der Enzyme). The costs of publication of this article were defrayed in part by the payment of page charges. This article must therefore be hereby marked "*advertisement*" in accordance with 18 U.S.C. Section 1734 solely to indicate this fact.

§ To whom correspondence should be addressed: Cytokine Biology and Genetics Programme, McClay Research Centre, School of Pharmacy, QUB, 97 Lisburn Rd., Belfast BT9 7BL, UK. Tel.: 44-2890-272214; Fax: 44-2890-247794, E-mail: k.vandenbroeck@qub.ac.uk.

** Recipient of a postdoctoral research fellowship from the Fonds voor Wetenschappelijk Onderzoek-Flanders.

¶¶ Supported by a Marie Curie fellowship.

[1] The abbreviations used are: IFN-γ, interferon-γ; HSP70, generic term for all members of the 70-kDa heat shock protein family; IL, interleukin; PVDF, polyvinylidene difluoride; RCMLA, reduced and carboxymethylated lactalbumin; IAANS, 2-(4-iodoacetamido)anilinonaphthalene-6-sulfonic acid; HIV, human immunodeficiency virus.

irreversible aggregation (14, 15). *In vitro* refolding conditions that resemble the physicochemical environment of the natural folding environment of IFN-γ, *i.e.* the endoplasmic reticulum, are not permissive for assembly of IFN-γ dimers, but result in aggregation (16). Thus, physiological temperatures and high concentrations of folding intermediates of IFN-γ appear to counteract spontaneous dimer formation. Third, support for a role of the endoplasmic reticulum DnaK homolog BiP/GRP78 in the *de novo* folding of IFN-γ comes from experiments in which IFN-γ-producing Chinese hamster ovary cells were transfected with a BiP ATPase mutant (T37G) that was previously shown to be able to bind peptide, but to be unable to release it upon binding of ATP (17). In co-immunoprecipitation experiments, mutant (but not wild-type) BiP formed a stable complex with IFN-γ. In addition, IFN-γ secretion was reduced from cells transfected with T37G BiP.[2]

To unravel the mechanistic basis of how chaperones may assist folding of IFN-γ, we have recently conducted a series of experiments using the *E. coli* chaperones GroEL/ES and DnaK/DnaJ/GrpE (16, 18). Both these chaperone systems have been thoroughly characterized, and the determinants of interaction with protein substrates are known. The DnaK chaperone and its HSP70 homologs, including the endoplasmic reticulum variant BiP/GRP78, bind preferentially to stretches of hydrophobic amino acids that are usually buried in the core of completely folded proteins, but exposed on unfolded or partially folded proteins (for review, see Ref. 19). This interaction prevents "off-pathway" misfolding normally leading to aggregation. Folding resumes after ATP-mediated substrate release from the chaperone, a reaction that is catalyzed by cofactors such as the nucleotide exchange factor GrpE. The mechanism of action of GroEL is different in that exposure of domains made up by αβ-folds with extensive hydrophobic surfaces is thought to be the driving force for interaction (20).

We assessed interaction of IFN-γ with both chaperone systems using recombinant IFN-γ samples that were previously denatured by either acid or heat (50 °C). Formation of tertiary structure was scored by a combination of methods, including enzyme-linked immunosorbent assay, antiviral bioassay, and SDS-PAGE. Under nonpermissive conditions for regain of tertiary structure (low ionic strength, 35 °C), the yield of correctly folded dimeric IFN-γ increased ~30-fold with GroEL/ES and ~20-fold with DnaK/DnaJ/GrpE above the level of spontaneous refolding starting from acid-unfolded protein (16, 18). In addition, GroEL/ES was shown to protect IFN-γ against thermal inactivation at 50 °C by binding to and arresting the aggregation of a thermal unfolding intermediate. This suggests that both *E. coli* chaperone systems can assist folding of IFN-γ in much the same way as they do with physiological substrates, *i.e.* by interacting with aggregation-prone conformers.

To further model the interaction between HSP70 chaperones and IFN-γ, we have now screened cellulose-bound peptide libraries derived from human and mouse IFN-γ for identification of DnaK-binding sites. This approach has been used successfully in the identification of DnaK-binding motifs from a variety of proteins (21, 22). Putative binding sites were confirmed by competition assays using soluble peptides. We report the identification of conserved functional DnaK-binding sites in α-helices B and C of human and mouse IFN-γ. These motifs are located at the dimer interface of IFN-γ. The helix C motif is specifically conserved among members of the superfamily of interleukin (IL)-10-related cytokines. Rüdiger *et al.* (22, 23) only rarely found DnaK-binding sites within sequences of dimerization interfaces that adopt helical structures in the native state. Our data therefore indicate that binding of DnaK to the helix C motif may be representative of an uncommon conserved regulatory mechanism in which HSP70-like chaperones mediate formation of the interdigitated hydrophobic folding interface in this class of homodimeric cytokines.

[2] K. Vandenbroeck and J. R. Gaut, unpublished data.

EXPERIMENTAL PROCEDURES

Screening of DnaK Binding to IFN-γ-derived Cellulose-bound Peptides by Fractionated Electroblotting—Peptide libraries consisting of 44 and 41 13-mer peptides covering the entire mature protein portions of human and mouse IFN-γ, respectively, were prepared by automated spot synthesis (24, 25). Peptides were attached through their C termini to a cellulose membrane via a $(\beta\text{-Ala})_2$ spacer (Jerini Bio Tools GmbH, Berlin, Germany). Analysis of DnaK binding was carried out essentially as described previously (21, 22). Briefly, peptide membranes were allowed to react with 100 nM DnaK (Stressgen Biotech Corp.) in buffer containing 31 mM Tris-HCl, pH 7.6, 170 mM NaCl, 6.4 mM KCl, 0.05% (v/v) Tween 20, and 5.0% (w/v) sucrose for 1 h at 25 °C with gentle shaking. Unbound DnaK was removed by washing three times with Tris-buffered saline (31 mM Tris-HCl, pH 7.6, 170 mM NaCl, and 6.4 mM KCl) at 4 °C. Electrotransfer of peptide-bound DnaK onto polyvinylidene difluoride (PVDF) membranes was performed using a semidry blotter. Cellulose and PVDF membranes were sandwiched between blotting paper soaked in anode buffer (anode buffer I: 30 mM Tris base and 20% MeOH; anode buffer II: 300 mM Tris base and 20% MeOH) and cathode buffer (25 mM Tris base, 40 mM 6-aminohexane acid, and 20% MeOH supplemented with increasing concentrations of SDS). Electrotransfer was performed at a constant power of 0.8 mA/cm^2. Cathode buffer was supplemented successively with 0.01, 0.1, and 0.5% SDS. At each cathode buffer change, new PVDF membranes were used. Transferred DnaK was detected with a mouse monoclonal anti-DnaK antibody (clone 8E2/2, Stressgen Biotech Corp.) using an ECL kit (Amersham Biosciences). Cellulose membranes contained three reference peptides (C1, C2, and C3), all of which have previously been shown to constitute good DnaK binders (21, 22), *i.e.* from hemagglutinin (Trp^{436}–Asn^{448}), peptide WTYNAELLVLLEN (indicated as C1); from alkaline phosphatase (Gly^{382}–His^{394}), peptide GNTLVIVTADHAH (indicated as C2); and from σ^{32} (Ser^{192}–Lys^{204}), peptide SHAMAPVLYLQDK (indicated as C3).

Peptide Synthesis—Peptides were synthesized on a Pioneer® instrument using standard solid-phase Fmoc (*N*-(9-fluorenyl)methoxycarbonyl) synthesis protocols. Alternatively, solid-phase peptide synthesis was performed on a Model 433A peptide synthesizer with conditional double coupling steps (Applied Biosystems, Foster City, CA). Each peptide was prepared as a C-terminal amide and was "capped" using acetic anhydride. All peptides were characterized using liquid chromatography/tandem mass spectrometry and purified by high pressure liquid chromatography.

Peptide Competition of Complex Formation between DnaK and Reduced and Carboxymethylated Lactalbumin (RCMLA)—Competition binding assays were performed as described (26, 27). 70 nM DnaK was incubated with 40 mM RCMLA for 2 h at 37 °C in buffer containing 25 mM Tris-HCl, 20 mM HEPES, pH 7.15, 47.5 mM KCl, and 2.25 mM $Mg(OAc)_2$ in the presence of competing peptide (0–500 μM). Free DnaK and DnaK·peptide complexes were separated from DnaK·RCMLA complexes by native PAGE on 6% acrylamide gels and visualized by immunoblotting with anti-DnaK antibody 8E2/2 using the ECL kit. All experiments were repeated at least three times.

σ^{32}-Q132-Q144-C-IAANS Competition Assay—The K_D values of peptides H10-9, M10-9, H44-9, and Rc2 for DnaK were determined by competition with an IAANS-labeled peptide (*E. coli* σ^{32}-Q132-Q144-C-IAANS) for binding to DnaK (21). DnaK (0.1 μM) and σ^{32}-Q132-Q144-C-IAANS (0.5 μM) were incubated with increasing concentrations of peptides H10-9 (0–20 μM), M10-9 (0–20 μM), H44-9 (0–60 μM), and Rc2 (0–40 μM) in 25 mM HEPES, pH 7.6, 50 mM KCl, and 10 mM $MgCl_2$ for 90 min at 30 °C. The fluorescence intensities ($F - F_{max}$) at an emission maximum of 452 nm (λ_{ex} = 335 nm) were plotted against the corresponding peptide concentrations and fitted (GRAPHIT 5.0.1) by a quadratic equation using the K_D of binding of σ^{32}-Q132-Q144-C-IAANS to DnaK (78 nM) (see Ref. 28). All experiments were repeated at least three times.

RESULTS

Screening of DnaK Binding to Peptide Libraries Derived from Human and Mouse IFN-γ—In a preliminary experiment, we analyzed the binding of DnaK to cellulose-bound peptides de-

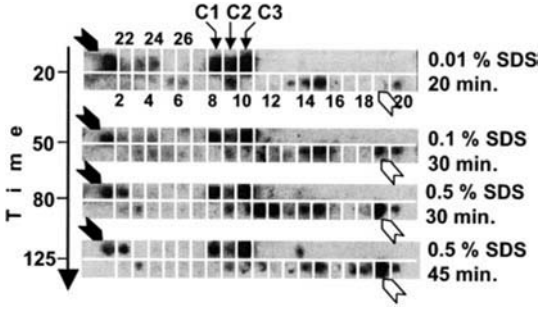

FIG. 1. **Effect of SDS concentration on electroelution of solid-phase peptide-bound DnaK.** DnaK was incubated with a cellulose membrane containing peptides derived from the C helices of human, mouse, and porcine IFN-γ. Peptide-bound DnaK was transferred onto PVDF membranes by fractionated electroblotting using cathode buffer supplemented successively with 0.01, 0.1, and 0.5% SDS and visualized with anti-DnaK antibodies and chemiluminescence. *Arrows* indicate the differential elution behavior of DnaK from two peptides: FYFKLFKNFKDDQ (*white arrows*) and FYLRLFEVLKDNQ (*black arrows*). The cellulose membrane contained three reference peptides (C1, C2, and C3; see "Experimental Procedures" for details), all of which have previously been shown to constitute good DnaK binders (22). SDS concentrations in cathode buffer and the corresponding time for each elution step are indicated on the right. The cumulative time for elution is indicated on the left.

rived from the hydrophobic C helices from human, mouse, and porcine IFN-γ. Peptide-bound DnaK was released by electroelution using cathode buffer supplemented successively with 0.01, 0.1, and 0.5% SDS. Under the conditions of the assay, release of DnaK from specific IFN-γ peptides appeared to be influenced by the concentration of SDS (Fig. 1). This is exemplified by the differential elution behavior of DnaK from peptides FYLRLFEVLKDNQ (from mouse IFN-γ; indicated by *black arrows* in Fig. 1) and FYFKLFKNFKDDQ (homologous peptide from human IFN-γ; indicated with *white arrows* in Fig. 1). Whereas cathode buffer supplemented with 0.01% SDS forced elution of >60% of DnaK from the first peptide, 0.5% SDS was required for quantitative elution of DnaK from the second peptide. These findings were taken into account in all further experiments in that electroelution was routinely carried out in three steps using cathode buffer supplemented successively with 0.01, 0.1, and 0.5% SDS. Rüdiger *et al.* (22) observed effects similar to those found in this study during the fractionated electrotransfer of DnaK from solid-phase bound peptides, even at constant SDS concentration. However, they optimized the conditions for their study to suppress this effect so as to obtain an averaged image in one blot. Therefore, the data obtained in both studies are comparable.

Cellulose-bound peptide libraries were used to scan human and mouse IFN-γ for the presence of DnaK-binding sites. The peptide scans consisted of 13-mer peptides overlapping by 10 amino acids, starting with the N terminus of the mature sequences. 44 peptides covered the human sequence, whereas the mouse sequence, which lacks the 9 C-terminal amino acids, was covered by 41 peptides. Because the hydrophobic core region in the DnaK-binding motif has a length of 4–5 amino acids, all potential linear DnaK-binding sites are thus logically represented in these libraries. Fig. 2 shows the results of the screen. Amounts of DnaK eluted stepwise with 0.01, 0.1, and 0.5% SDS-supplemented cathode buffer were approximated by densitometry and added up. Three reference peptides (C1, C2, and C3) previously shown to constitute good DnaK binders (21, 22) were included in each membrane. To ensure that the binding of DnaK to any of the cellulose-bound peptides was specific, an additional experiment was carried out in which a soluble competitor substrate peptide, *i.e.* peptide BH801 (sequence YWWNLLQ) derived from HIV gp160, was added during incubation of the membrane with DnaK. This peptide has previously been shown to display high affinity for DnaK (27). Its inclusion in the incubation buffer severely reduced binding of DnaK to membrane-bound peptides (data not shown). This suggests that the interaction of DnaK with cellulose-bound peptides occurs mechanistically through the substrate recognition site.

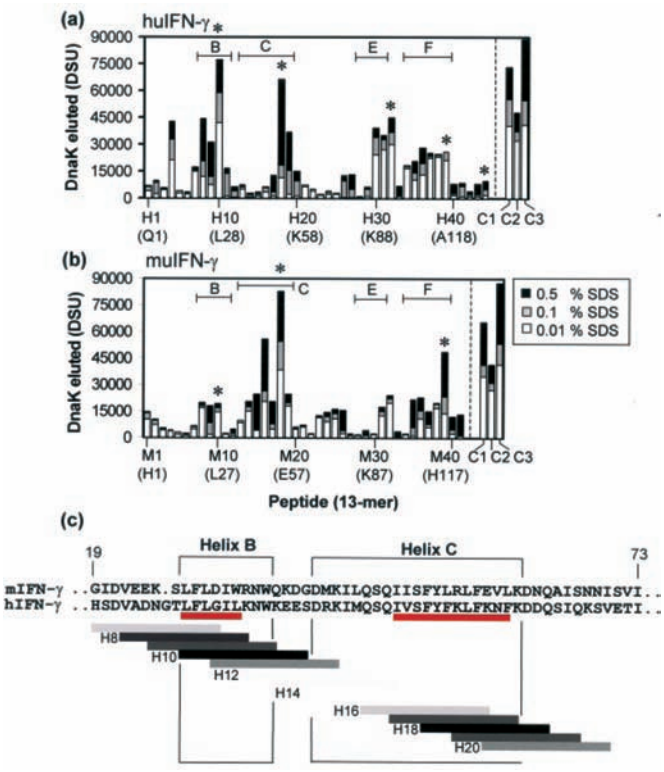

FIG. 2. **Identification of DnaK binding sites in IFN-γ.** *a* and *b*, analysis of the binding of DnaK to solid-phase peptide libraries of human (*huIFN-γ*) and mouse (*muIFN-γ*) IFN-γ, respectively. Results of one experiment of three performed are shown. Peptides (13-mers) start with the N termini of the mature IFN-γ portions and scan the entire sequences toward the C terminus, moving along by 3 amino acids, thus yielding an overlap window of 10 residues. Membranes were incubated with DnaK, followed by fractionated electrotransfer of peptide-bound DnaK to PVDF membranes. Cathode buffer was supplemented successively with 0.01, 0.1, and 0.5% SDS. The amount of eluted DnaK was quantified by densitometry of immunoblots. Each cellulose membrane contained the three reference peptides (C1, C2, and C3), described in the legend to Fig. 1. *Asterisks* denote solid-phase peptides from which 9-mer peptides were derived for analysis in the RCMLA and/or σ^{32}-Q132-Q144-IAANS competition assays. (9-mers were derived from the overlap windows of DnaK-binding (*i.e.* peptides H10, H18, H32, M18, and M39) or homologous (*i.e.* peptides M10 and H39) regions; peptides H43 and H44 did not show apparent binding of DnaK, but were theoretically predicted to contain a DnaK-binding site (see Fig. 6).) Relevant α-helices are indicated at the top (B, C, E, and F). *c*, a portion of human IFN-γ encompassing helices B and C, shown aligned with corresponding 13-mer peptides from the peptide scan. The average of the pooled amount of DnaK eluted with 0.01, 0.1, and 0.5% SDS-supplemented cathode buffer from these peptides in three experiments is approximated by the *shade* of the *bars*. Predicted DnaK-binding core sites in the human sequence are *underlined* in *red*. For reference, the corresponding sequence from mouse IFN-γ (*mIFN-γ*) is also given aligned with that from human IFN-γ (*hIFN-γ*). *DSU*, densitometric scanning unit.

The Amount of DnaK Eluted from IFN-γ-derived Cellulose-bound Peptides Correlates with DnaK-Peptide Affinity Measured in the RCMLA Assay—Upon consideration of the total amount of DnaK eluted, at least two major and several minor DnaK-binding sites in both human and mouse IFN-γ can be inferred (Fig. 2). Some peptides appeared to bind limited amounts of DnaK, although subsequent elution required high

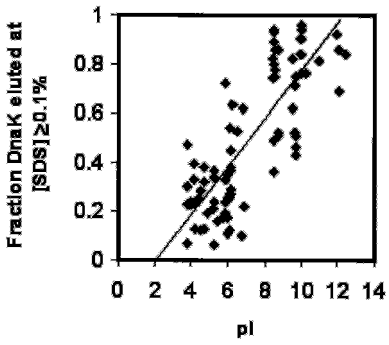

FIG. 3. **Plot of the fraction of DnaK eluted with ≥0.1% SDS against the isoelectric points of all 88 peptides from Fig. 2 (r = 0.81, t = 12.69, degrees of freedom = 86).**

concentrations of SDS (≥0.1%) in cathode buffer, *e.g.* all peptides corresponding to the C termini of human and mouse IFN-γ (peptides H41–H44 for human IFN-γ and peptides M40 and M41 for mouse IFN-γ). All of these peptides contain polybasic sequences (KRKR in peptides H41–H43, RGRR in peptide H44, and RKRK in peptides M40 and M41), raising the possibility that lack of elution of DnaK with 0.01% SDS might be due to reinforcement of hydrophobic interactions by added electrostatic effects. Indeed, regression analysis of the fraction of DnaK eluted with ≥0.1% SDS against the isoelectric points of all 88 peptides from Fig. 2 revealed a linear correlation (r = 0.81, t = 12.69, degrees of freedom = 86, $p < 10^{-10}$) (Fig. 3). The fraction or total quantity of DnaK eluted with ≥0.1% SDS did not correlate with aliphatic index or grand average of hydropathicity of these peptides (data not shown).

Further indications that the amount of DnaK eluted with ≥0.1% SDS is to be taken into account when estimating affinity on the basis of the solid-phase assay came from subsequent analysis of soluble peptides in the RCMLA assay (Table I and Fig. 4). This is a competition assay in which soluble peptides are tested for their ability to compete with an unfolded form of lactalbumin (RCMLA) (see Ref. 26) for binding to DnaK over a range of concentrations (0–500 μM). Nine 9-mer peptides were synthesized that were derived from the overlap windows of weak, intermediate, and strong binders as inferred from the solid-phase assay. Apparent affinity for DnaK (K_{app}) (see Ref. 27) was measured as the peptide concentration yielding 50% inhibition of binding of RCMLA to DnaK. HIV gp160-derived peptide BH801 (YWWNLLQ), the K_{app} of which in the RCMLA assay has previously been determined to be 50 μM (27), was used as a positive control and was included in each assay (Table I and Fig. 4). The amount of DnaK eluted from peptides in the solid-phase assay was found to be indicative of the affinity measured in the RCMLA assay (see below for correlation analysis).

However, a discrepancy was observed between the interactions of peptide M10-9 (LFLDIWRNW) with DnaK in the RCMLA *versus* solid-phase assay (in the latter of which this peptide constitutes the overlap of peptides M9 and M10). Although this peptide displayed a strong affinity for DnaK in the former assay (K_{app} = 10 μM), it bound only a small quantity of DnaK in the solid-phase assay. The homologous peptide in human IFN-γ, H10-9 (LFLGILKNW), did not display this anomalous behavior, as it showed strong affinities for DnaK in both assays. To clarify this issue, we used another competition assay for determination of affinity. In this assay, the K_D values of the binding affinity of both peptides M10-9 and H10-9 for DnaK were measured by competition with σ^{32}-Q132-Q144-C-IAANS for binding to DnaK (21). Up to 12 concentrations of competing peptide were used centering around the inhibitory concentration (IC_{50}) (Fig. 5). This assay yielded K_D values of 0.12 ± 0.02 μM for peptide H10-9 and 0.25 ± 0.02 μM for peptide M10-9, thus identifying both peptides as truly very strong DnaK binders.

We investigated whether the relationship between the amounts of DnaK eluted from peptides in the solid-phase assay and the affinities of their core motifs for DnaK as determined in the RCMLA assay could be formalized by linear regression analysis. Of the nine IFN-γ-derived peptides tested (Table I), we omitted peptide M10-9 because of its anomalous behavior. We observed a significant inverse correlation between the K_{app} obtained for each of the remaining 9-mer peptides and the pooled amount of DnaK eluted with 0.01, 0.1, and 0.5% SDS from their solid phase counterparts (r = −0.91, p = 0.005). Upon consideration of the amount of DnaK eluted with ≥0.1% SDS only, the correlation with K_{app} values became slightly stronger (r = −0.92, p = 0.004).

α-Helices B and C of Mouse and Human IFN-γ Contain Conserved High-affinity DnaK-binding sites—The combined data from the solid-phase screening and from the RCMLA and σ^{32}-Q132-Q144-C-IAANS competition assays indicate the location of conserved high-affinity DnaK-binding sites in the N-terminal half of helix B and the C-terminal half of helix C of human and mouse IFN-γ (Table I). We used an algorithm based on the experimental screening of the binding of DnaK to 4360 peptides to localize more precisely the DnaK-binding core motifs in these helices (22). The most probable motif for interaction of DnaK with helix B was confined to a 6-amino acid stretch consisting of two overlapping 5-residue cores (L^{28}FLGIL) (energy value less than −10; values less than −5 are likely to be DnaK binders (see Ref. 22)). In helix C, a 12-amino acid stretch consisting of six overlapping core motifs with energy values less than −6 was identified (I^{49}VSFYFKLFKNF) (Fig. 2*c*). Within this stretch, the core motifs I^{49}VSFY and Y^{53}FKLF had the lowest energy values of –9 and –10, respectively, and thus the highest predicted affinity for DnaK. As shown above, these helix B and C motifs as part of 9-mer peptides bound DnaK with high affinity (Table I and Figs. 4 and 5). In each of these homologs, the helix B and C DnaK substrate regions are separated by a stretch of 15 amino acids. An additional DnaK motif was identified in helix F of mouse IFN-γ (R^{114}VVHQLLPE; K_{app} = 80 μM) that seems not to be functionally conserved in the human form (homologous position Q^{115}VMAELSPA; K_{app} = 400 μM).

In general, the experimental findings corroborate the theoretical prediction of DnaK sites in human and mouse IFN-γ. For instance, as shown in Fig. 6 the conserved DnaK-binding sites in helices B and C as well as the helix F motif in mouse IFN-γ were correctly predicted. A binding site was theoretically predicted to occur in the C terminus of human IFN-γ (Q^{133}MLFRGR; energy value of −10) that did not show up in the solid-phase assay (peptides H42 and H43) (Fig. 2) and neither in the RCMLA assay (K_{app} > 500 μM for peptide H44-9) (Table I and Fig. 4). However, the K_D of this peptide as measured in the σ^{32}-Q132-Q144-C-IAANS competition assays was 3.6 μM. This value is smaller than the recently determined cutoff value of 7 μM for the K_D, above which peptide substrates are anticipated not to stimulate ATP hydrolysis and hence not to bind to DnaK (28). Thus, with the present data, it is difficult to exclude a role for this site in HSP70 chaperone-assisted folding of IFN-γ.

Implications for Folding of IFN-γ—With the high-resolution (1.4 Å) three-dimensional structure for human IFN-γ being available (code 1fg9; Protein Data Bank), we attempted to infer the implications of the localization of the two conserved DnaK-binding sites in helices B and C for the folding of the dimer

TABLE I
Interactions between DnaK and peptides derived from IFN-γ, IL-20, and IL-24/FISP

Peptide	Protein	Location	Peptide sequence	DnaK binding		
				DnaK eluted[a]	K_{app}[b]	K_D[c]
				DSU	*μM*	*μM*
H10–9	huIFN-γ[d]	Helix B	LFLGILKNW	77,000	<10	0.12 ± 0.02
M10–9	muIFN-γ	Helix B	LFLDIWRNW	19,000	10	0.25±0.02
H18–9A	huIFN-γ	Helix C	IVSFYFKLF	66,000	40	ND
H18–9B	huIFN-γ	Helix C	FYFKLFKNF	66,000	30	ND[e]
M18–9	muIFN-γ	Helix C	FYLRLFEVL	85,000	<10[f]	ND[e]
H32–9	huIFN-γ	Helix E	KLTNYSVTD	45,000	400	ND
H39–9	muIFN-γ	Helix F	QVMAELSPA	25,000	400	ND
M39–9	muIFN-γ	Helix F	RVVHQLLPE	48,000	80	ND
H44–9	huIFN-γ	CT	RSQMLFRGR	5,000	>500	3.6 ± 1.2
4αHC	huIL-20	Helix C	HLLRLYLDRVF	ND	15	ND
Rc1	muIL-24/FISP	Helix C	SLLKFYLNTVF	ND	60	ND
Rc2	muIL-24/FISP	Helix C	LLKFYLNTV	ND	40	1.03 ± 0.4
BH801[g]	HIV gp160	CP	YWWNLLQ	ND	40	ND

[a] Total amount of DnaK electroeluted with 0.01, 0.1, and 0.5% SDS from solid-phase peptides approximated by anti-DnaK immunoblotting and densitometric scanning.
[b] K_{app} is defined as the concentration of peptide necessary for half-maximum competition of DnaK binding to RCMLA.
[c] K_D was determined by competition of unlabeled peptides with σ^{32}-Q132-Q144-C-IAANS for binding to DnaK (21).
[d] hu, human; mu, murine; CT, C terminus; CP, cytoplasmic domain; ND, not determined; DSU, densitometric scanning unit.
[e] K_D values of peptides H18–9B and M18–9 could not be determined due to aggregation.
[f] Peptide M18–9 aggregated/caused aggregation of DnaK at concentrations above 20 μM in the RCMLA assay.
[g] BH801 was used as reference peptide. (K_{app} in the DnaK/RCMLA assay was previously determined at 50 μM (see Ref. 27)).

(Figs. 7 and 8). The helix B and C DnaK motifs exhibit significant solvent accessibility (helix B motif, 617 Å (monomer) and 327 Å (dimer); and helix C motif, 625 Å (monomer) and 410 Å (dimer)). The decrease in going from the monomer to the dimer is due to the presence of helices E and F of the second subunit packing against helices B and C of the first. It is interesting to note that the helix B and C portions encompassing DnaK sites have a very similar patch of solvent-accessible surface (Fig. 8). This is centered on a lysine residue in both cases (L^{30}–$K^{34}N^{35}$ for helix B and F^{54}–$K^{58}N^{59}$ for helix C). Taking into account structural constraints imposed by the second domain of IFN-γ that is adjacent to the helix C motif, it seems that, in the folded dimer, the helix B (but not the helix C) chaperone motif might be exposed to macromolecular access. This could be of importance for invoking a role for HSP70-like chaperones in the prevention of irreversible thermal inactivation through "early" interaction with the helix B motif, *i.e.* before thermally induced unfolding of the dimer exposes the helix motif C for interaction with chaperones. Figs. 7 and 8 show that, toward the interior of the dimer, the helix B and C DnaK-binding sites interact at their N termini within each subunit (F^{29}–$F^{52}Y^{53}$), showing the normal "edge-to-face" alignment of aromatic rings, and with Leu^{113} in helix F of the second subunit. The hydrophobic surface created by $F^{52}Y^{53}$ (donated by the helix C motif) and Leu^{28} (from the helix B motif) from the first subunit forms a small pocket filled by the C-β of Ala^{109} from helix F of the second subunit (29). Helix F shows a pronounced bend of ~55–60° centered on Glu^{112}, which is unique to IFN-γ, IL-10, and related cytokines (29–31). Leu^{28}, Phe^{52}, Tyr^{53}, Ala^{109}, and Glu^{112} are conserved in IL-10 and IFN-γ and cluster with extensive contacts in the core of the dimer around the bend in helix F. These 5 amino acids are thought to represent key residues in stabilizing the IFN-γ/IL-10 typical structural fold (29). The donation of the first 3 residues by high-affinity DnaK-binding sites (Leu^{28} by the helix B motif and $F^{52}Y^{53}$ by the helix C motif) advocates a role for HSP70-like chaperones in *de novo* positioning, stabilization, or prevention of flawed alignment of this IFN-γ/IL-10 typical fold.

The DnaK-binding Motif in α-Helix C of IFN-γ Is Conserved in the Superfamily of Interleukin-10-related Cytokines—A number of novel IFN-γ/IL-10 homologs have recently been identified, including IL-19 (32), IL-20 (33), IL-22 (34, 35), and

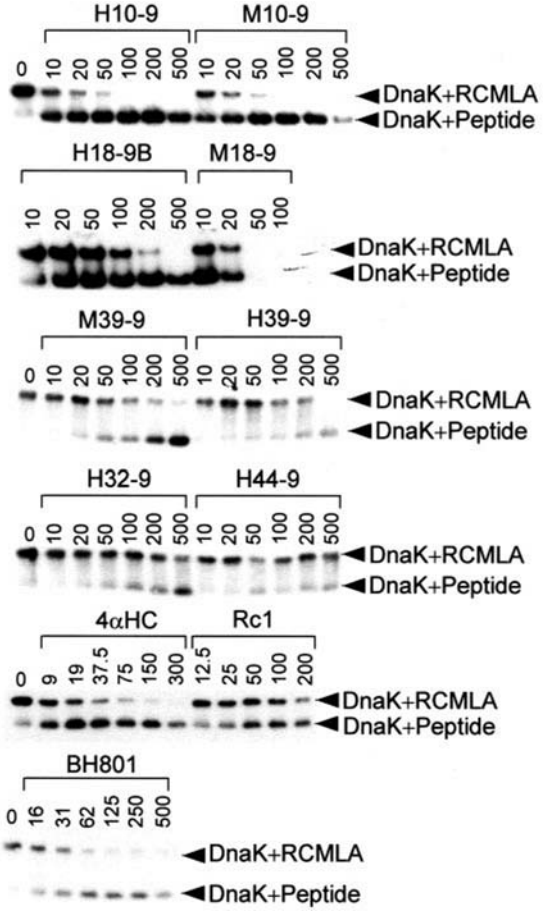

FIG. 4. **Competition of complex formation between DnaK and RCMLA by soluble peptides.** 70 nM DnaK (50 ng/assay) was incubated with 40 μM RCMLA in the absence or presence of increasing concentrations of competing peptide (0–500 μM). Free DnaK and DnaK·peptide complexes were separated from DnaK·RCMLA complexes by native PAGE (6% polyacrylamide) and visualized by blotting, followed by detection with anti-DnaK antibodies. Peptide BH801 (YWWNLLQ) derived from HIV gp160 was used as a reference peptide (27) and was included in each experiment. The results of one of three experiments performed are presented. The sequences of the peptides tested are given in Table I.

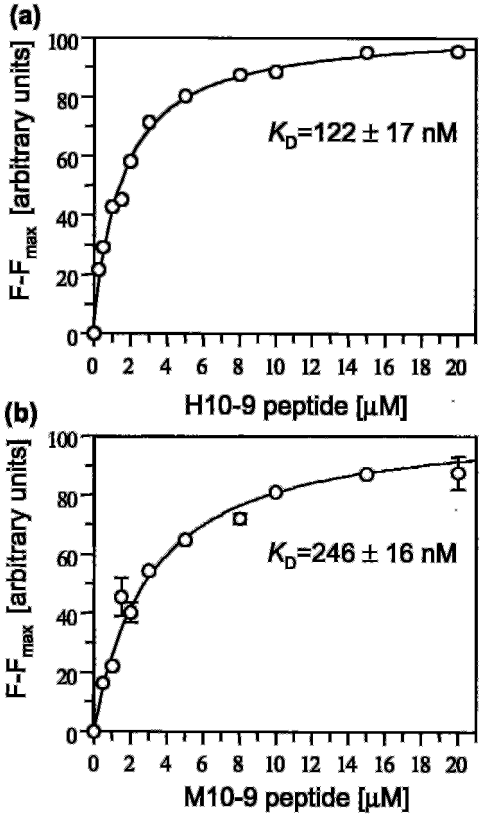

FIG. 5. **Determination of the affinity of peptides for DnaK.** *a* and *b*, titration of peptides H10-9 (helix B from human IFN-γ) and M10-9 (helix B from mouse IFN-γ), respectively, against DnaK and σ^{32}-Q132-Q144-C-IAANS (full sequence, QRKLFFNLRKTKQ) for determination of K_D. The fluorescence ($F - F_{max}$) was plotted against the corresponding peptide (H10-9 and M10-9) concentration. Complex formation between DnaK and σ^{32}-Q132-Q144-C-IAANS in the absence of competing peptide yielded the highest fluorescence intensity (F_{max}). Values are averaged over three independent experiments. Peptides H44-9 and Rc2 (see Table I) were also processed in this assay (not shown).

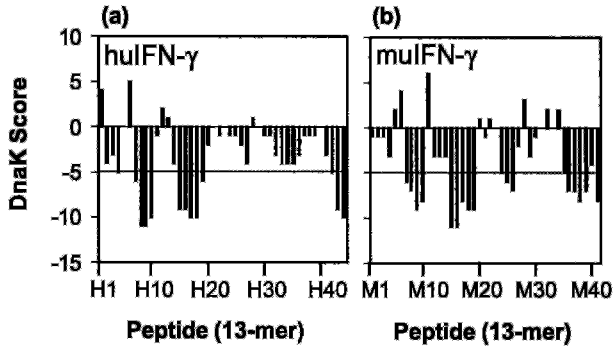

FIG. 6. **Prediction of DnaK-binding sites in the primary structures of the mature portions of human (*a*) and mouse (*b*) IFN-γ.** Each of the *bars* represents the predicted score for binding of DnaK to a single 13-mer peptide from the original peptide scans shown in Fig. 2. Scores were calculated with the algorithm described by Rüdiger *et al.* (22). Peptide numbering corresponds to that shown in Fig. 2 (control peptides C1, C2, and C3 were excluded). The *dotted lines* indicate the cutoff value set at –5 (corresponding to an experimentally verified correct level of prediction of binding sites of 82%). *huIFN-γ*, human IFN-γ; *muIFN-γ*, mouse IFN-γ.

IL-26/AK155 (36). Also MDA-7 (37), rat C49a/MOB-5 (38, 39), and mouse interleukin-4 induced secreted protein (40) belong to this superfamily and were recently renamed as IL-24 (41). More distantly related viral IL-10 homologs have been identified in the genomes of rhesus, simian, and human cytomegalovirus (42, 43); lumpy skin disease virus (44); and Yaba-like disease virus (45).

Alignment of 55 members of this superfamily unveiled two regions of extensive conservation (Fig. 9). The first region of conservation was found in helix C around the DnaK substrate region identified in IFN-γ (70% consensus motif, *phlp*FYL*c*); the second region is composed of amino acids around the pronounced bend in helix F seen in the crystal structures of IFN-γ and IL-10 (70% consensus motif, KA*hp*E*h*). The likelihood for occurrence of DnaK sites in helices C and F was calculated using the DnaK site prediction algorithm (22). No DnaK-binding sites were predicted in the conserved helix F region. In helix C, a conserved 6-residue stretch (consensus, *hlp*FYL) was predicted to constitute the core of a DnaK-binding site in IFN-γ, IL-19, IL-20, IL-22, IL-24, and IL-26 (Fig. 9). However, the corresponding sequences in IL-10 and most viral IL-10 homologs were predicted to be non-binders, essentially due to the clustering of negatively charged residues in the regions flanking the core motif, which are likely to disfavor binding to DnaK (22, 23).

To experimentally verify the validity of this calculation, we tested interaction between DnaK and the theoretically predicted helix C motifs in two members of this family, *i.e.* motifs HLLRLYLDRVF from human interleukin-20 and SLLKFYLNTVF present in rat and mouse IL-24, by the RCMLA competition assay (Table I and Fig. 4). Both peptides were indeed identified as strong DnaK binders, yielding K_{app} values of 15 and 60 μM, respectively, suggesting functional conservation of the helix C chaperone-binding site in this superfamily of cytokines. The nonapeptide core motif LLKFYLNTV derived from rat and mouse IL-24 bound to DnaK with strong affinity (K_D = 1 μM) in the σ^{32}-Q132-Q144-C-IAANS competition assay, further confirming this site as a potential natural target for HSP70 chaperone interaction.

DISCUSSION

In this work, we provide evidence for the presence of two high-affinity DnaK-binding sites in α-helices B and C of interferon-γ. In addition, nonconserved lower affinity binding sites were putatively identified in helix F of mouse IFN-γ and in the C terminus of human IFN-γ. Upon consideration of all peptides showing at least some degree of DnaK binding in the solid-phase assay (Fig. 2), it seems that the occurrence of sites sustaining a minimal level of interaction with DnaK is enriched in and largely confined to only those α-helices that contribute to the interlocking dimer interface (constituted by the helix B-loop II-helix C and helix E-loop V-helix F segments) (4, 5). Thus, helices A and D can reasonably be excluded as potential targets for chaperone interaction. Of notable interest is the finding that the helix C motif appears to be conserved in the majority of cytokines belonging to the IL-10 superfamily.

We used three complementary approaches for identification of these sites, *i.e.* screening of libraries of solid-phase bound peptides scanning human and mouse IFN-γ, quantification of suppression by soluble IFN-γ-derived peptides of complex formation between DnaK and RCMLA, and analysis of the competition of some of these peptides with σ^{32}-Q132-Q144-C-IAANS for binding to DnaK. An interesting finding is that the amount of DnaK eluted from solid-phase peptides correlated inversely with the K_{app} of their core peptides in the RCMLA assay ($r = -0.91$, $p = 0.005$). Furthermore, of the four peptides that were processed in the σ^{32}-Q132-Q144-C-IAANS assay, the K_D values correlated with their K_{app} values as measured in the RCMLA assay ($r = 0.98$, $p = 0.02$). Although, because of the limited number of peptides tested, caution is warranted when interpreting these results, this suggests that the quantity of DnaK eluted from peptides in the solid-phase assay could be

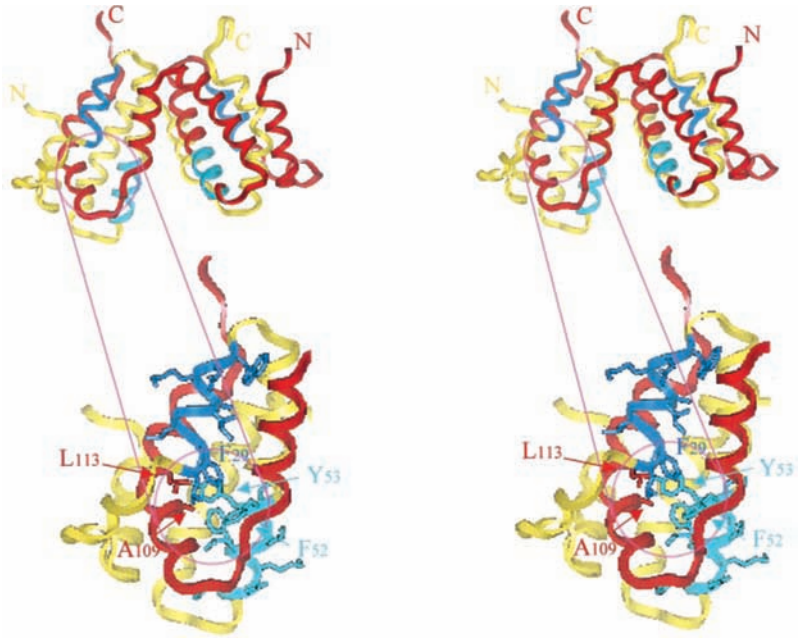

FIG. 7. **Location of DnaK-binding sites in the IFN-γ dimer.** Stereo ribbon diagrams show the locations of high-affinity DnaK-binding motifs in α-helices B (*blue*) and C (*cyan*) in the IFN-γ dimer (code 1fg9; Protein Data Bank). The *lower parts* represent magnified diagrams of the interaction between Phe^{29}, Phe^{52}, and Tyr^{53} of these motifs in the first subunit and Ala^{109} and Leu^{113} located around the bend in helix F in the second subunit of IFN-γ (code 1fg9). *Yellow* and *red ribbons* correspond to the distinct monomers in the dimer.

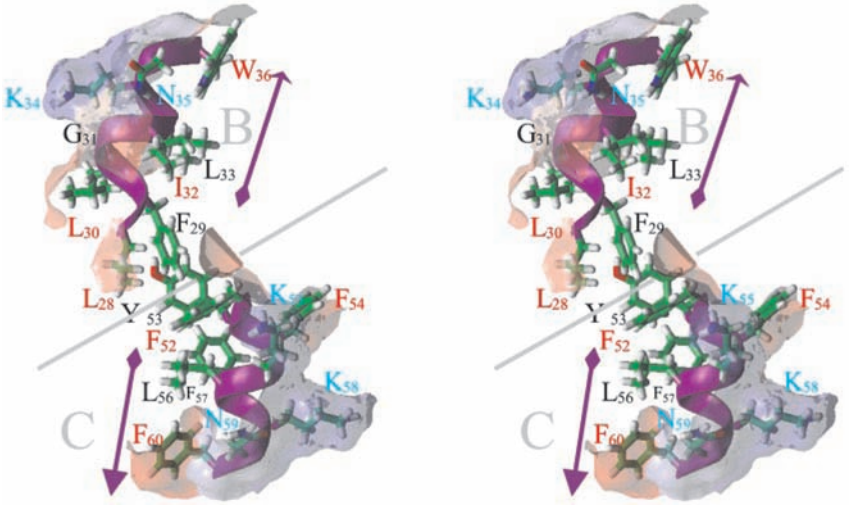

FIG. 8. **Molecular modeling of DnaK-binding sites in α-helices B and C of IFN-γ.** Shown is a stereo view of the solvent-accessible area, location, and interaction of DnaK-binding motifs in α-helices B and C of human IFN-γ. Only the side chains of Leu^{28}–Trp^{36} (helix B, upper region; *B*) and Phe^{52}–Phe^{60} (helix C, lower region; *C*) are shown from one subunit of the dimer in the crystal structure of human IFN-γ (code 1fg9; Protein Data Bank). The *diagonal gray lines* divide the two motifs, and the *purple arrows* show the orientation of the two helices (*diamonds* at the N-terminal ends). The helix fold is represented as a *ribbon* (*purple*). A semitransparent solvent-accessible surface is also displayed, with hydrophobic regions in *red* and hydrophilic regions in *blue*. Individual residues are labeled in one of three colors: *red* for solvent-accessible hydrophobic, *blue* for solvent-accessible hydrophilic, and *black* for either buried residues or an exposed glycine.

applied as a predictive measure for estimating the affinity of interaction of these peptides with DnaK. However, it should be noted that the interaction of DnaK with peptide M10-9 (LFLDIWRNW) in soluble form differed quantitatively from that seen in the solid-phase assay (overlap of peptides M9 and M10). Although this peptide was identified as a strong DnaK binder in both RCMLA and σ^{32}-Q132-Q144-C-IAANS competition assays, it bound only a small amount of DnaK in the solid-phase assay. These findings are congruent with earlier observations that quantitative differences between peptides in solution and cellulose-bound peptides might occur. An explanation for this divergence might be sought in the unusually high activation entropy of substrate binding to DnaK (46). The entropy of a given peptide in soluble form differs from that in solid-phase form and is also different from the positional context in the whole protein. However, the enthalpic terms should be comparable, thus substantiating the notion that the observed differences are quantitative, but not qualitative.

The DnaK motifs identified in this study conform to the proposed binding motif consisting of 4–5 hydrophobic amino acids enriched for Leu, Ile, Val, Phe, and Tyr with basic residues adjacent to the hydrophobic core (22, 47). The high-affinity DnaK motifs identified in this study are all located in peptide segments that adopt an α-helical conformation in the folded protein. This is remarkable in view of the finding that helical structures were reported not to fit into the substrate-binding cleft of DnaK (47). The majority of good DnaK-binding sites localize preferentially to β-strands of corresponding folded proteins, even if it is known that peptide segments with intrinsic propensity to form α-helical structures can bind DnaK as long as they occur in an extended (*i.e.* unfolded) conformation (22, 23). IFN-γ may therefore constitute an uncommon example of a high-affinity all-α-helical HSP70 substrate. Especially the identification of a functional DnaK site in helix C of IFN-γ and

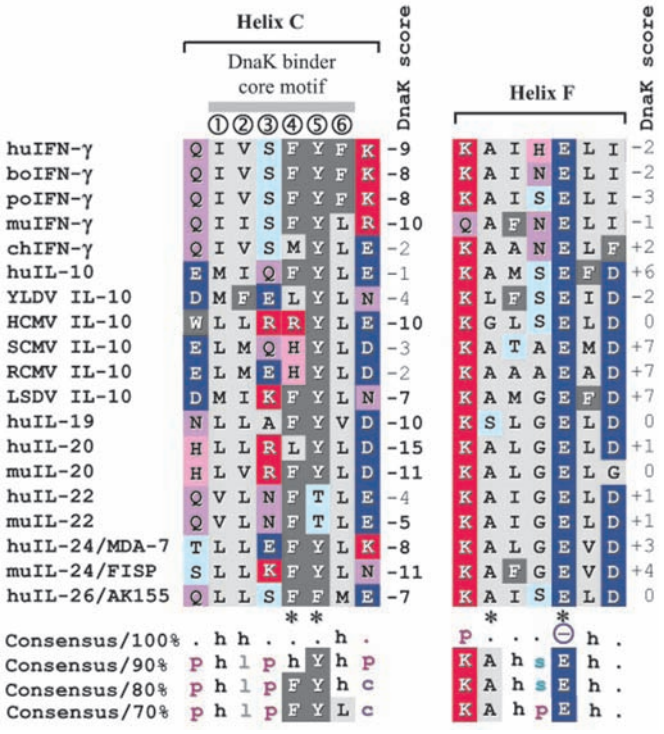

FIG. 9. **DnaK-binding sites are predicted to occur in the structurally conserved helix C (but not F) of cytokines belonging to the IFN-γ/IL-10 superfamily.** The location of the 6-residue DnaK-binding core motif in helix C is indicated with a *horizontal gray bar*. As the probability of binding to DnaK is determined by the differential energy contributions of each amino acid in a 5-residue core and two 4-residue flanking regions, combined energy values were calculated for the sequences shown, taking into account additional flanking amino acids (not shown). Scores are represented in *boldface* if less than or equal to −5 (cutoff corresponding to an experimentally verified correct prediction level of binding of 82%). Conserved amino acid sequences at consensus levels of 100, 90, 80, and 70% are based on a total of 55 proteins, including those shown and, in addition, 18 mammalian and avian IFN-γ proteins and 18 mammalian and viral IL-10 proteins. Four of the 5 conserved amino acids (Phe^{52}, Tyr^{53}, Ala^{109}, and Glu^{112} in human IFN-γ) clustering around the bend in helix F originally identified in the three-dimensional structures of human IFN-γ and IL-10 by Walter and Nagabhushan (29) are indicated with *asterisks*. The remaining residue (Leu^{28}) is located in helix B (not shown). Coloring reflects physicochemical properties of residues: *c*, charged; *h*, hydrophobic; *l*, aliphatic; *p*, polar; *s*, small; −, negatively charged. *hu*, human; *bo*, bovine; *po*, porcine; *mu*, murine; *ch*, chicken; *YLDV*, Yaba-like disease virus; *HCMV*, human cytomegalovirus; *SCMV*, simian cytomegalovirus; *RCMV*, rhesus cytomegalovirus; *LSDV*, lumpy skin disease virus; *FISP*, interleukin-4 induced secreted protein.

IL-10-related cytokines may further the understanding of the role of chaperones in protein folding. Helix C is the longest and most hydrophobic helix and is buried in the core of the dimer (4, 5). Essentially, the IFN-γ dimer interface is centered on a pair of two symmetry-related C helices (4). In their survey of homodimeric proteins, Larsen *et al.* (10) identified a small class of interfaces that have subunits that interdigitate extensively and that exhibit the strongly hydrophobic character of the interior core of a single-chain folded domain. This led them to conclude that, for these proteins, the entire dimer forms in one folding step, rather than from association of two individually folded subunits. This type of protein folding is most accurately represented with a two-state folding model in which the two chains fold cooperatively, and stable intermediate monomers tend not to occur (48). Larsen *et al.* (10) distinguished two functional classes in this category of proteins, *i.e.* DNA-binding proteins (*e.g. arc* and *trp* repressors) and cytokines (*e.g.* IFN-γ and IL-10). Analysis of the folding of the α-helical *trp* repressor supports the two-state model for this category of proteins, as this protein exhibits a folding pathway in which the intersubunit hydrophobic core first forms and only subsequently the flanking structures (49, 50). Thermal denaturation studies of IFN-γ substantiate a dimer formed as a single cooperative thermodynamic domain, with dimerization being mandatory for generation of tertiary structure (51). To our knowledge, the role of chaperones in folding of this category of proteins has not been investigated in detail. The functional conservation of a DnaK-binding motif in helix C at the dimer interface suggests that, at least in the cytokines IFN-γ, IL-19, IL-20, IL-22, IL-24, and IL-26, HSP70-like chaperones might be directly involved in assembly of the dimer by inhibiting unproductive side reactions at this stage. In support of this concept are the findings of Kendrick *et al.* (9), who, using solution thermodynamic approaches, found that only a slight expansion of the surface area of the IFN-γ dimer is needed to form an aggregation-prone conformer. With the IFN-γ dimer interface accounting for up to 40% of the total surface area, this finding implies a transient native-like dimer (rather than a dimer-monomer) transition involved in off-pathway aggregation. If relevant for *de novo* folding, this would invoke a role for HSP70 chaperones in suppressing aggregation of this dimer form of IFN-γ. This model is in contrast with the majority of dimers that fold through a three-state model (48), for which subunit folding and formation of hydrophobic nuclei and hence concomitant interaction with HSP70 chaperones are likely to be completed before the dimerization step.

An additional DnaK-binding site was putatively identified in the C terminus of human IFN-γ. The K_D of this motif (RSQML-FRGR) was 3.6 μM. This value is in the same order of magnitude as that previously found for the heat shock transcription factor σ^{32}, a physiological substrate for DnaK (21). Because the cutoff value for binding to DnaK has been determined at a K_D of 7 μM (28), it is thus possible that this site represents a true substrate for HSP70 chaperones. However, if so, this motif may be of lesser significance, as it was not evolutionarily conserved in rodent IFN-γ due to the absence of the 9 C-terminal amino acids. The C terminus of human IFN-γ was not observed in the original crystal structure (4), but is supposed to be flexible in solution (52). Landar *et al.* (53) determined the crystal structure of a single-chain mutant of IFN-γ with an intact C terminus (IFNγSC1). The C-terminal sequence QMLFRG was modeled in a hydrophobic binding pocket formed by two non-crystallographically related IFN-γSC1 molecules. Although it is not certain whether this interaction is representative for the soluble state, the finding that this motif coincides exactly with a DnaK-binding site may argue for a buried (rather than solvent-exposed) location of the C terminus.

In the natural folding compartment of IFN-γ, the endoplasmic reticulum, it is likely that it is the DnaK homolog BiP/GRP78 that will interact with any of the motifs determined in this study. Even though minor differences in substrate recognition have been suggested (26, 54), BiP and DnaK binding patterns are generally conserved, and both chaperones recognize similar side chains (55). Attempts in our laboratory to screen the IFN-γ peptide libraries for binding to BiP failed (data not shown), probably due to the fact that the peptide affinity of BiP has been shown to be 1–2 orders of magnitude lower than that of DnaK (56, 57). However, by co-immunoprecipitation experiments, we have been able to demonstrate interaction of BiP/GRP78 with IFN-γ,[2] suggesting a functional role for this chaperone in *de novo* folding of IFN-γ.

This work may contribute to a better understanding of the processes regulating folding and secretion of this therapeutically important class of cytokines. Josephson *et al.* (58) recently presented compelling evidence for a novel ligand-receptor rec-

ognition paradigm in which IL-10 receptor-1 and receptor-2 share the same binding site on IL-10. Remarkably, 3 amino acids of the contact interface with the receptor appear to be conserved in the whole superfamily of IL-10-related cytokines, including IFN-γ. Two of these are the Lys and Glu residues found near the bend in helix F (Fig. 9). The structure of the IFN-γ·IFN-γ receptor-1 complex revealed that IFN-γ receptor-1 interacts in a virtually identical way with this conserved residue cluster on IFN-γ (59). Our work indicates that the amino acid sequence around and including the highly conserved $F^{52}Y^{53}$ motif in helix C of this superfamily is probably mandatory for chaperone-assisted generation of the IFN-γ/IL-10 typical fold. Thus, pending future investigation, we propose that both the mechanisms determining regulation of folding and ligand-receptor interaction occur along the same lines in this class of cytokines.

REFERENCES

1. Billiau, A. (1996) *Adv. Immunol.* **62,** 61–130
2. Marsters, S. A., Pennica, D., Bach, E., Schreiber, R. D., and Ashkenazi, A. (1995) *Proc. Natl. Acad. Sci. U. S. A.* **92,** 5401–5405
3. Bach, E. A., Tanner, J. W., Marsters, S., Ashkenazi, A., Aguet, M., Shaw, A. S., and Schreiber, R. D. (1996) *Mol. Cell. Biol.* **16,** 3214–3221
4. Ealick, S. E., Cook, W. J., Vijay-Kumar, S., Carson, M., Nagabhushan, T. L., Trotta, P. P., and Bugg, C. E. (1991) *Science* **252,** 698–701
5. Samudzi, C. T., Burtoni, L. E., and Rubin, J. R. (1991) *J. Biol. Chem.* **266,** 21791–21797
6. Sprang, S. R., and Bazan, J. F. (1993) *Curr. Biol.* **3,** 815–827
7. Bennett, M. J., Schlunegger, M. P., and Eisenberg, D. (1995) *Protein Sci.* **4,** 2455–2468
8. Xu, D., Tsai, C.-J., and Nussinov, R. (1998) *Protein Sci.* **7,** 533–544
9. Kendrick, B. S., Carpenter, J. F., Cleland, J. L., and Randolph, T. W. (1998) *Proc. Natl. Acad. Sci. U. S. A.* **95,** 14142–14146
10. Larsen, T. A., Olson, A. J., and Goodsell, D. S. (1998) *Structure* **6,** 421–427
11. Arakawa, T., Hsu, Y.-R., and Yphantis, D. A. (1987) *Biochemistry* **26,** 5428–5432
12. Mulkerrin, M. G., and Wetzel, R. (1989) *Biochemistry* **28,** 6556–6561
13. Kendrick, B. S., Cleland, J. L., Lam, X., Nguyen, T., Randolph, T. W., Manning, M. C., and Carpenter, J. F. (1998) *J. Pharm. Sci.* **87,** 1069–1076
14. Arakawa, T., Alton, N. K., and Hsu, Y.-R. (1985) *J. Biol. Chem.* **260,** 14435–14439
15. Vandenbroeck, K., Martens, E., D'André, S., and Billiau, A. (1993) *Eur. J. Biochem.* **215,** 481–486
16. Vandenbroeck, K., Martens, E., and Billiau, A. (1998) *Eur. J. Biochem.* **251,** 181–188
17. Wei, J. Y., Gaut, J. R., and Hendershot, L. M. (1995) *J. Biol. Chem.* **270,** 26677–26682
18. Vandenbroeck, K., and Billiau, A. (1998) *Biochimie* (*Paris*) **80,** 729–737
19. Gottesman, M. E., and Hendrickson, W. A. (2000) *Curr. Opin. Microbiol.* **3,** 197–202
20. Houry, W. A., Frishman, D., Eckerskorn, C., Lottspeich, F., and Hartl, F. U. (1999) *Nature* **402,** 147–154
21. McCarty, J. S., Rüdiger, S., Schönfeld, H.-J., Schneider-Mergener, J., Nakahigashi, K., Yura, T., and Bukau, B. (1996) *J. Mol. Biol.* **256,** 829–837
22. Rüdiger, S., Germeroth, L., Schneider-Mergener, J., and Bukau, B. (1997) *EMBO J.* **16,** 1501–1507
23. Rüdiger, S., Buchberger, A., and Bukau, B. (1997) *Nature Struct. Biol.* **4,** 342–349
24. Frank, R. (1992) *Tetrahedron* **48,** 9217–9232
25. Kramer, A., Schuster, A., Reineke, U., Malin, R., Volkmer-Engert, R., Landgraf, C., and Schneider-Mergener, J. (1994) *Methods Comp. Methods Enzymol.* **6,** 388–395
26. Fourie, A. M., Sambrook, J. F., and Gething, M.-J. (1994) *J. Mol. Biol.* **269,** 30470–30478
27. Knarr, G., Modrow, S., Todd, A., Gething, M.-J., and Buchner, J. (1999) *J. Biol. Chem.* **274,** 29850–29857
28. Mayer, M. P., Schröder, H., Rüdiger, S., Paal, K., Laufen, T., and Bukau, B. (2000) *Nature Struct. Biol.* **7,** 586–593
29. Walter, M. R., and Nagabhushan, T. L. (1995) *Biochemistry* **34,** 12118–12125
30. Zdanov, A., Schalk-HiHi, C., Gustchina, A., Tsang, M., Weatherbee, J., and Wlodawer, A. (1995) *Structure* **3,** 591–601
31. Zdanov, A., Schalk-HiHi, C., Menon, S., Moore, K. W., and Wlodawer, A. (1997) *J. Mol. Biol.* **268,** 460–467
32. Gallagher, G., Dickensheets, H., Eskdale, J., Izotova, L. S., Mirochnitchenko, O. V., Peat, J. D., Vazquez, N., Pestka, S., Donnelly, R. P., and Kotenko, S. V. (2000) *Genes Immun.* **1,** 442–450
33. Blumberg, H., Conklin, D., Xu, W. F., Grossmann, A., Brender, T., Carollo, S., Eagan, M., Foster, D., Haldeman, B. A., Hammond, A., *et al*. (2001) *Cell* **104,** 9–19
34. Dumoutier, L., Louahed, J., and Renauld, J.-C. (2000) *J. Immunol.* **164,** 1814–1819
35. Xie, H.-H., Aggarwal, S., Ho, W.-H., Foster, J., Zhang, Z., Stinson, J., Wood, W. I., Goddard, A. D., and Gurney, A. L. (2000) *J. Biol. Chem.* **275,** 31335–31339
36. Knappe, A., Hor, S., Wittman, S., and Fickenscher, H. (2000) *J. Virol.* **74,** 3881–3887
37. Jiang, H., Su, Z.-Z., Lin, J. J., Goldstein, N. I., Young, C. S. H., and Fisher, P. B. (1996) *Proc. Natl. Acad. Sci. U. S. A.* **93,** 9160–9165
38. Soo, C., Shaw, W. W., Freymiller, E., Longaker, M. T., Bertolami, C. N., Chiu, R., Tieu, A., and Ting, K. (1999) *J. Cell. Biochem.* **74,** 1–10
39. Zhang, R., Tan, Z. J., and Liang, P. (2000) *J. Biol. Chem.* **275,** 24436–24443
40. Schaefer, G., Venkataraman, C., and Schindler, U. (2001) *J. Immunol.* **166,** 5859–5863
41. Fickenscher, H., Hör, S., Küpers, H., Knappe. A., Wittmann, S., and Sticht, H. (2002) *Trends Immunol.* **23,** 89–96
42. Kotenko, S. V., Saccani, S., Izotova, L. S., Mirochnitchenko, O. V., and Pestka, S. (2000) *Proc. Natl. Acad. Sci. U. S. A.* **97,** 1695–1700
43. Lockridge, K. M., Zhou, S. S., Kravitz, R. H., Johnson, J. L., Sawai, E. T., Blewett, E. L., and Barry, P. A. (2000) *Virology* **268,** 272–278
44. Tulman, E. R., Afonso, C. L., Lu, Z., Zsak, L., Kutish, G. F., and Rock, D. L. (2001) *J. Virol.* **75,** 7122–7130
45. Lee, H. J., Essani, K., and Smith, G. L. (2001) *Virology* **281,** 170–192
46. Farr, C. D., Galiano, F. J., and Witt, S. N. (1995) *Biochemistry* **34,** 15574–15582
47. Zhu, X. T., Zhao, X., Burkholder, W. F., Gragerov, A., Ogata, C. M., Gottesman, M. E., and Hendrickson, W. A. (1996) *Science* **272,** 1606–1614
48. Tsai, C.-J., and Nussinov, R. (1997) *Protein Sci.* **6,** 1426–1437
49. Gittelman, M. S., and Matthews, C. R. (1990) *Biochemistry* **29,** 7011–7020
50. Taysaco, M. L., and Carey, J. (1992) *Science* **255,** 594–597
51. Dudich, I. V., Zavyalov, V. P., Bumyalis, V. A. V., and Paulauskas, D. V. (1992) *Mol. Biol.* **26,** 342–351
52. Grzesiek, S., Dobeli, H., Gentz, R., Garotta, G., Labhardt, A. M., and Bax, A. (1992) *Biochemistry* **31,** 8180–8190
53. Landar, A., Curry, B., Parker, M. H., DiGiacomo, R., Indelicato, S. R., Nagabhushan, T. L., Rizzi, G., and Walter, M. R. (2000) *J. Mol. Biol.* **299,** 169–179
54. Gragerov, A., and Gottesman, M. E. (1994) *J. Mol. Biol.* **241,** 133–135
55. Flynn, G. C., Pohl, J., Flocco, M. T., and Rothman, J. E. (1991) *Nature* **353,** 726–730
56. Flynn, G. C., Chappell, T. G., and Rothman, J. E. (1989) *Science* **245,** 385–390
57. Blond-Elguindi, S., Cwirla, S. E., Dower, W. J., Lipshutz, R. J., Sprang, S. R., Sambrook, J. F., and Gething, M.-J. H. (1993) *EMBO J.* **75,** 717–728
58. Josephson, K., Logsdon, N. J., and Walter, M. R. (2001) *Immunity* **14,** 35–46
59. Walter, M. R., Windsor, W. T., Nagabhushan, T. L., Lundell, D. J., Lunn, C. A., Zavodny, P. J., and Narula, S. K. (1995) *Nature* **367,** 230–235